

A Practical Phase Gate for Producing Bell Violations in Majorana Wires

David J. Clarke, Jay D. Sau, and Sankar Das Sarma

*Department of Physics, Condensed Matter Theory Center, University of Maryland,
College Park, Maryland 20742, USA and Joint Quantum Institute, University of Maryland,
College Park, Maryland 20742, USA*

(Received 9 October 2015; published 8 April 2016)

Carrying out fault-tolerant topological quantum computation using non-Abelian anyons (e.g., Majorana zero modes) is currently an important goal of worldwide experimental efforts. However, the Gottesman-Knill theorem [1] holds that if a system can only perform a certain subset of available quantum operations (i.e., operations from the Clifford group) in addition to the preparation and detection of qubit states in the computational basis, then that system is insufficient for universal quantum computation. Indeed, any measurement results in such a system could be reproduced within a local hidden variable theory, so there is no need for a quantum-mechanical explanation and therefore no possibility of quantum speedup [2]. Unfortunately, Clifford operations are precisely the ones available through braiding and measurement in systems supporting non-Abelian Majorana zero modes, which are otherwise an excellent candidate for topologically protected quantum computation. In order to move beyond the classically simulable subspace, an additional phase gate is required. This phase gate allows the system to violate the Bell-like Clauser-Horne-Shimony-Holt (CHSH) inequality that would constrain a local hidden variable theory. In this article, we introduce a new type of phase gate for the already-existing semiconductor-based Majorana wire systems and demonstrate how this phase gate may be benchmarked using CHSH measurements. We present an experimentally feasible schematic for such an experiment using a “measurement-only” approach that bypasses the need for explicit Majorana braiding. This approach may be scaled beyond the two-qubit system necessary for CHSH violations, leading to a well-defined platform for universal fault-tolerant quantum computation using Majorana zero modes.

DOI: [10.1103/PhysRevX.6.021005](https://doi.org/10.1103/PhysRevX.6.021005)

Subject Areas: Condensed Matter Physics,
Quantum Physics, Quantum Information

I. INTRODUCTION

Implementing fault-tolerant quantum computation using physical qubits is now a goal of many laboratories all over the world. Unique among such experimental efforts is so-called topological quantum computation (TQC), which utilizes exotic non-Abelian quasiparticles in storing the qubits. These anyons, the most prominent examples of which are zero-energy localized excitations (called “Majorana zero modes”) in the superconducting gaps of certain types of topological superconductors, are neither fermions nor bosons, obeying instead non-Abelian statistics in two-dimensional systems. As nonlocal topological objects, these anyonic quasiparticles are immune to local perturbations in the system and are thus characterized by highly suppressed quantum decoherence [3,4], making them, in some sense, ideal from the perspective of storing quantum information. Similarly, protected unitary operations may be performed with these anyons by adiabatically moving them

around one another (“braiding” them) to take advantage of the non-Abelian statistics. In the current work, we propose a compelling practical resolution of one of the most crucial conceptual roadblocks in carrying out anyonic TQC by providing a blueprint for how to carry out *universal* quantum computation using Majorana qubits. In the process, we also connect the anyonic TQC with fundamental aspects of quantum nonlocality, proposing the observation of a particular variant of the Bell inequality using Majorana zero modes as a clear signal of the universality of the underlying topological quantum computing platform.

Universal quantum computation requires the operator to have the ability to produce *any* quantum state in the computational Hilbert space, including, in particular, those that violate the limits imposed on local hidden variable theories by the Bell inequality [5] or its variants such as the Clauser-Horne-Shimony-Holt (CHSH) inequality [6]. Even with the aid of measurement, however, a topological quantum computer based on the braiding of anyonic Majorana fermion zero modes (MZMs) cannot create such a state in a topologically protected manner [3,4]. This is intimately related to the fact that the braids and measurements of MZMs together form a representation of the Clifford group [4,7–12], which is classically simulable [1]. This well-known

Published by the American Physical Society under the terms of the Creative Commons Attribution 3.0 License. Further distribution of this work must maintain attribution to the author(s) and the published article's title, journal citation, and DOI.

limitation of MZMs in carrying out universal quantum computations arises from the Ising [or $SU(2)_2$] nature of the corresponding topological quantum field theory (TQFT), which enables only $\pi/2$ rotations in the Hilbert space of the qubits through braiding. (The surface code implementation in superconducting qubits [13], which is turning out to be one of the most promising practical approaches to quantum computation at the present time [14], also suffers from the limitation of only supporting Clifford group operations in a natural way.)

While there are many theoretical proposals [15–19] for going beyond MZMs (i.e., beyond the Ising anyon universality) which, in principle, could lead to universal topological quantum computation by utilizing richer TQFT, e.g., $SU(2)_3$ or Fibonacci anyons, no such system has been experimentally demonstrated. Furthermore, these richer systems enabling universal TQC often require extremely complicated braiding operations involving very high overhead in order to approximate Clifford group operations [20], which themselves are useful for quantum error-correcting codes [21]. It is therefore of great importance to explore ideas that specifically utilize MZMs (with some additional operations) to carry out inherently quantum-mechanical tasks beyond the constraint of the Gottesman-Knill theorem.

In particular, it is well known that the “protected” operations of braiding and measurement on MZMs (and also the surface code) become universal for quantum computation when supplemented with a single-qubit phase gate of small enough angle [4,7–12,22]. The so-called $\pi/8$ phase gate (or T gate) $e^{-i\pi/8}|0\rangle\langle 0| + e^{i\pi/8}|1\rangle\langle 1|$ is often named as part of a universal gate set. In part, this is because of the “magic state distillation” [23] protocol that corrects errors in noisy T gates through the use of Clifford gates and measurement. However, any phase gate with $\theta \neq n\pi/4$ with n integer is sufficient for universal quantum computation as long as it can be produced consistently. (In fact, it would be useful for the reduction of overhead to be able to produce a phase gate of arbitrary angle, and there are now error-correction algorithms designed with this in mind [24].)

In this paper, we introduce a method for adiabatically performing the phase gate necessary to complement the existing Clifford operations and allow universal quantum computation with Majorana systems. In order to test such a gate, we propose what we believe to be the simplest nontrivial quantum demonstration feasible with MZMs, namely, violations of CHSH-Bell inequality. Furthermore, we show that the design used for the testing of the inequality leads directly to a practical platform for performing universal TQC with Majorana wires in which explicit braiding need never occur. Thus, our work involves three synergistically connected aspects of anyonic TQC (in the context of the currently active area of using MZMs for topological quantum computation): proposing a practical phase gate for universal topological quantum computation using MZMs, providing a precise protocol (using CHSH

inequality) for testing that the desired gate operation has been achieved, and bypassing the necessity of MZM braiding (and so avoiding, e.g., problems of nonadiabaticity in the braids [25]).

In designing the phase gate and the quantum computation platform, we take a “black-box” approach to the Majorana wire system itself, avoiding, as much as possible, the manipulation of parameters that might change the topological nature of the wire state, or tune couplings between the MZMs. We find this approach advantageous because of the still-developing nature of the Majorana field—the “best” wire platform may be yet to be proposed. We focus instead on a universal aspect of the Majorana system: a well-developed degeneracy associated with the fermion parity of a given wire. Remarkably, this approach (based in “measurement-only” TQC [26,27]) is entirely sufficient for producing and testing the adiabatic phase gate and (by extension) for universal quantum computation.

In Sec. II, we review the CHSH inequalities in the context of Majorana zero-mode physics. A measurement of violations of the CHSH-Bell inequalities is an important step in demonstrating not only the fundamental quantum physics and non-Abelian statistics of Majorana zero modes, but also the departure from the Clifford group that is necessary for universal quantum computation. In particular, it has been shown [28] that operations capable of producing a violation of the CHSH inequality, when combined with Clifford operations, are sufficient for universal quantum computation. This may be thought of as a refinement of the usual error-correction bound given by magic-state distillation [23]. Put another way, if a phase gate produces a violation of the CHSH inequalities, then it falls within the error-correction bound. Thus, a CHSH measurement may be used as a single-number benchmark of the quality of a gate, rather than relying on tomography of the entire produced state.

In Secs. III and IV, we introduce and analyze a new type of phase gate. Previous proposals [4,7,9,11,22,29–32] for introducing a single-qubit phase gate into a Majorana-wire-based system are fundamentally limited by timing errors due to the largely unknown relaxation rates involved in the detailed wire physics. We bypass these limitations by eliminating timing errors entirely, instead performing the phase gate adiabatically. This phase gate uses elements already present in the Hyart *et al.* proposal for braiding and Majorana-based memory [33] (semiconductor Majorana wires, superconductors, magnetic fields, and Josephson junctions), and so may be integrated into such a design without much additional overhead. For this reason, we use a design appropriate for incorporation into such a system in our analysis. However, the concept behind our phase gate is not limited to this specific setting, and its analog should be available in any Majorana wire system.

In Sec. V, we lay out our suggested experimental setup for benchmarking the new phase gate using the CHSH

inequalities. One great practical advantage of our proposal is that it builds on the existing proposals [33–37] for carrying out MZM braiding in semiconductor nanowire systems, which are currently being implemented in various laboratories on InSb and InAs nanowires [38,39]. In contrast to the various exotic proposals for going beyond MZMs and $SU(2)_2$ TQFT [15–19,40–42], our proposal does not necessitate building new experimental platforms but uses the already-existing and extensively experimentally studied semiconductor nanowire-based MZM platforms [7–12]. Importantly, the experiment we propose would unequivocally establish the non-Abelian nature of the Majorana zero modes, as well as testing the phase gate, and measurement-based experiments directly equivalent to Majorana braiding [26,27] could be performed in the same architecture. In fact, our system may provide a simpler platform for (effectively) braiding with nanowire MZMs than existing proposals [33–37] in the sense that no coupling needs to be fine-tuned between the various Majorana modes.

In Sec. VI, we construct a scalable memory register capable of measuring any Pauli operator on a set of qubits. This architecture requires only one junction of Majorana wires per qubit, greatly simplifying fabrication requirements for a Majorana-wire platform. Combined with the phase gate of Sec. III, this design would enable universal fault-tolerant quantum computation using nanowire MZMs. We note that we have designed this device with elements in mind that are available now, but the principles behind our phase gate and memory design should be adaptable to any future Majorana wire system.

II. CHSH INEQUALITIES

To begin, we discuss the device-independent aspects of our proposal, as the protocol we describe to test the CHSH inequalities is independent of the particular platform used to realize MZMs (and, as such, transcends the specific Majorana wire system of current experimental interest we focus on later in the paper). In order to test the inequality, we require a minimum of six Majorana zero modes, the ability to do a pairwise measurement of adjacent Majorana modes, and a phase gate implemented on (a particular) two of the Majorana modes. The procedure is as follows:

First, we divide our six MZMs into two sets of three (see Fig. 1). We label the Majorana fermion operators associated with the zero modes as α_i and β_i , where $i \in \{1, 2, 3\}$. The eigenvalues and commutation relations of the operators $i\alpha_i\alpha_j$ are such that we can make the identification

$$i\epsilon_{ijk}\alpha_i\alpha_j \equiv 2\sigma_k^*, \quad (1)$$

where the σ_k are Pauli matrices. The complex conjugation on the right-hand side reverses the sign of σ_2 and ensures the correct commutation relations. In this way, we can identify the operators of three MZMs with those of a single spin- $\frac{1}{2}$, such that the pairwise measurement of the state of

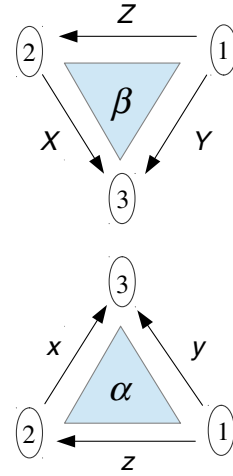


FIG. 1. This figure shows six Majorana zero modes arranged in two qubits consisting of three MZMs each, with pairs corresponding to the x , y , and z axes of each qubit labeled. An arrow designates the definition of the corresponding Pauli operator in terms of the MZMs. For example, $\sigma_z = i\alpha_1\alpha_2$, $\sigma_y = i\alpha_1\alpha_3$.

two of the three MZMs corresponds to a projective measurement along the x , y , or z axis of the spin. We have labeled these pseudospin axes in Fig. 1. We define Pauli matrices for the β_i operators similarly and label the axes there with capital letters.

The CHSH-Bell inequality [6] now asserts that, in particular,

$$E(x, X) - E(x, Z) + E(z, X) + E(z, Z) \leq 2 \quad (2)$$

for a local hidden variable theory, where $E(a, B)$ indicates the expectation value of the operator $a \otimes B$. Local in this case means local to the qubits, i.e., sets of three MZMs. The measurements we are making are necessarily *nonlocal* in the individual MZMs themselves.

That said, one may prepare a state that violates the CHSH inequality by first making initialization measurements that entangle the state of the two qubits. To this end, we begin by measuring the operators $i\alpha_1\beta_1$ and $i\alpha_2\beta_2$, projecting both into their -1 eigenstates [43]. Surprisingly, this alone is not enough to violate the inequality but only to saturate it. In spin language, in the z basis, we are in the state $\frac{1}{\sqrt{2}}(|\uparrow\uparrow\rangle + |\downarrow\downarrow\rangle)$. One may easily check that the expectation value of $x \otimes X - x \otimes Z + z \otimes X + z \otimes Z$ for this state is indeed 2. In fact, any set of measurements (or braiding) we do on the MZMs can only saturate the classical bound, never exceed it (thus not manifesting quantum entanglement properties, as is consistent with the Gottesmann-Knill theorem). To violate the CHSH inequality, we must add a phase gate (or equivalent) to the system. Applying this gate around the y axis with an angle θ , we find that

$$\begin{aligned}
 & E(x, X) - E(x, Z) + E(z, X) + E(z, Z) \\
 & = 2\sqrt{2} \cos(2\theta - \pi/4).
 \end{aligned} \tag{3}$$

Note that the phase gate that is available from braiding alone has $\theta = \pi/4$ and therefore can only saturate the classical bound (2). A more finely resolved phase gate than is available from braiding is necessary in order to violate the CHSH inequality. We discuss below how this can be done in a simple manner in order to directly observe quantum entanglement properties through the violation of CHSH-Bell inequality in a MZM-based platform.

III. PHASE GATE

There are now several proposals for introducing the necessary phase gate into a Majorana-based quantum computing scheme, including bringing the MZMs together in order to split the degeneracy for some time period [4,7,9,11], using the topological properties of the system to create such a splitting nonlocally [29–32], or transferring the quantum information to a different kind of qubit in order to perform the gate [44]. Of these, the third requires a separate control scheme for the additional qubit, while the first two rely crucially on timing. In this paper, we present a new type of phase gate whose elements are native to the Majorana wire platform and which performs the phase rotation adiabatically so that precise timing is not a concern. The phase gate builds on previous proposals [29,30,45] that use the topological properties of the system in a non-topologically-protected way in order to produce the gate [46]. However, the fact that it is only a slight variation on already-existing experimental setups [47–53] should presumably make our proposal easier to implement.

We begin by considering the following thought experiment: Two Majorana zero modes (or Ising anyons) together form a two-level system, which we may think of as the σ_z component of a qubit. A third Ising anyon will pick up a topological component of phase $\pi(1 - \sigma_z)/2$ upon going past this pair around the top, relative to the phase it picks up going around the bottom, in addition to any Abelian phase (see Fig. 2). If instead of giving this particle a classical trajectory, we allow it to behave quantum mechanically, then it now has some complex amplitude A (or B) for going above (or below) the qubit pair as it moves from left to right. The total left-to-right amplitude is $A\sigma_z + B$. In the special case that the (Abelian) phases of A and B differ by $\chi = 90^\circ$, the transmission probability is independent of the qubit state, and a phase gate

$$\begin{aligned}
 U(A, B) &= \frac{1}{\sqrt{|A|^2 + |B|^2}} (|B\rangle + i|A\rangle\sigma_z) \\
 &= e^{i \arctan[(|A|)/(|B|)] \sigma_z}
 \end{aligned} \tag{4}$$

is applied to the qubit by the passage of the anyon. In order to realize this concept in a more physical (i.e., experimental)

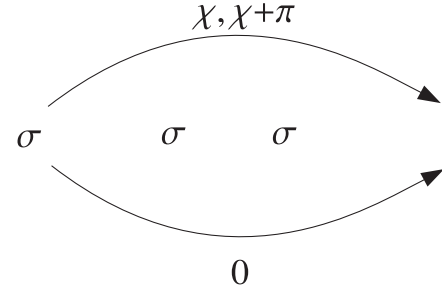


FIG. 2. This figure shows the phase gained by an Ising anyon passing above or below a stationary Ising pair. The phase acquired is dependent on the combined state (qubit) stored by the two anyons. If the test particle passes entirely to one side of the pair, it acquires a topological phase of 0 or π relative to passing on the other side, in addition to the Abelian phase χ . Quantum effects, whereby the test particle has an amplitude to pass on either side and these paths interfere, can lead to more general (though unprotected) phases. The role of the test particle in our proposal is played by a Josephson vortex, while that of the stationary pair is held by a Majorana wire placed on a superconducting island.

setting, we consider a ring of superconducting islands connected by three Josephson junctions (Fig. 3). Two of the Josephson junctions will be adjustable, while the third is assumed to be a much stronger link than the other two. One of these islands will hold a Majorana wire of the type described by Refs. [54–56], which has already been the subject of experimental studies [47–53]. The endpoints of

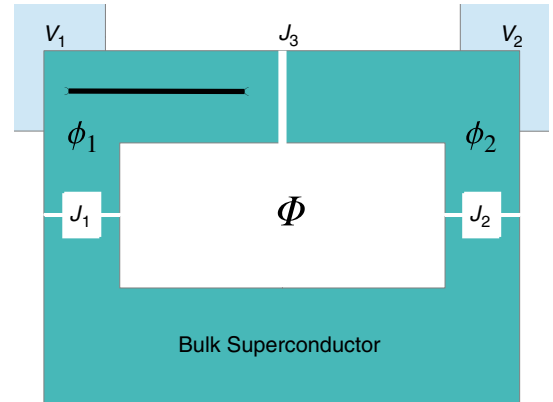


FIG. 3. Proposed device for implementing a phase gate. A Majorana nanowire sits on the upper left of two superconducting islands connected to a bulk superconductor. Josephson junctions J_1 and J_2 are adjustable, while a Josephson junction J_3 is strong and fixed. Gates of potential V_1 and V_2 are capacitively coupled to the superconducting islands. Operation of the phase gate is performed by ramping up the flux in the superconducting loop from $\Phi = 0$ to $\Phi = 2\pi$, while the strengths of couplings J_1 and J_2 are comparable to draw a Josephson vortex into the loop through two interfering paths, then ramping the flux back down to zero with $J_2 \ll J_1$ to release the vortex deterministically through the right junction.

this wire act as Majorana zero modes and allow that island to contain either an even or odd number of electrons with no energy penalty. We use the fermion parity ($q = \{0, 1\}$) of this island as the axis of the qubit around which we perform our rotation. The role of the mobile Ising anyon in the above proposal may then be played by a magnetic flux vortex traveling through the Josephson junctions to enter the ring. The topological component of the phase picked up when a flux encircles the Majorana wire is again $\pi(1 - \sigma_z)/2$, now arising from the Aharonov-Casher effect [30,31,57–60]. Finally, our setup includes a capacitive coupling to an adjustable gate voltage to one or both of the superconducting islands. This is represented in our model by the “gate charge” vector $\vec{Q} = (C_{g1}V_{g1} \ C_2V_{g2})$, where C_{gi} and V_{gi} are, respectively, the capacitance and voltage of the gates on each island. Changing \vec{Q} allows us to adjust the relative (Abelian) phase χ acquired by the flux as it moves through one or the other of the weak Josephson links.

In order to implement our phase gate, we adjust the external magnetic field to slowly (adiabatically) increase the amount of magnetic flux running through the superconducting loop from 0 to 2π . (Note that there is no precise constraint on the exact timing of the flux-threading process as long as it is adiabatic.) This adjustment will deterministically draw a Josephson vortex into the loop through one of the weak links, but crucially, it does not measure which path that vortex takes. This is exactly the anyon interferometer we need to produce the phase gate [45].

It remains to determine the phase that is produced based on the physical parameters of the system. To do so, we begin with the Lagrangian

$$L = \frac{1}{2} \left(\frac{\Phi_0}{2\pi} \right)^2 \dot{\vec{\phi}} C \dot{\vec{\phi}} + \frac{\Phi_0}{2\pi} \dot{\vec{\phi}} \cdot (\vec{Q}^T + e\vec{q}^T) - V(\phi_1, \phi_2), \quad (5)$$

where $\vec{\phi} = (\phi_1 \ \phi_2)$, $C = \begin{pmatrix} C_1 & -C_3 \\ -C_3 & C_2 \end{pmatrix}$, and

$$V(\phi_1, \phi_2) = -J_1 \cos(\phi_1 - \Phi/2) - J_2 \cos(\phi_2 + \Phi/2) - J_3 \cos(\phi_1 - \phi_2). \quad (6)$$

Here, $\vec{q} = (q \ 0)$ is the fermion parity on the Majorana wire, the variable Φ is the flux through the superconducting ring, and $\dot{\phi}_i$ is the time derivative of the superconducting phase on island i .

To run our phase gate, we adiabatically increase the value of Φ from 0 to 2π by applying an external magnetic field (Fig. 4). We are most interested in the point $\Phi = \pi$, at which the system will need to cross a tunnel barrier to move from one degenerate minimum (the true minimum for $\Phi < \pi$) to the other (the true minimum for $\Phi > \pi$) (see Fig. 5). We consider a system for which

$$J_3(J_1 + J_2) \geq J_1J_2 \geq J_3(J_1 - J_2) \geq 0. \quad (7)$$

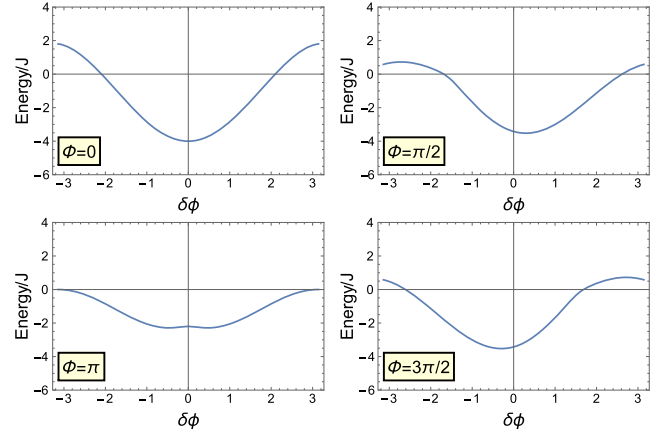


FIG. 4. Potential energy vs the superconducting phase difference $\delta\phi = \phi_1 - \phi_2$ [minimized over $\bar{\phi} = (\phi_1 + \phi_2)/2$], plotted for a junction twice as strong as the average of the other two ($\lambda = 2$) and a Josephson asymmetry $\epsilon = 0.1$, and various values of Φ . As Φ is tuned from 0 to 2π , a magnetic flux is drawn into the superconducting loop. Note the degeneracy at $\Phi = \pi$.

In such a system, the tunneling is well described by two interfering paths. Both paths will alter the phase difference $\delta\phi = \phi_1 - \phi_2$ by the same amount. The paths differ by a full 2π winding of the average phase $\bar{\phi} = (\phi_1 + \phi_2)/2$ of the superconducting islands.

When $\Phi = \pi$, the degenerate minima of the potential V occur at

$$\begin{aligned} \cos(\delta\phi) &= \frac{J_1^2 + J_2^2}{2J_1J_2} - \frac{J_1J_2}{2J_3^2}, \\ \tan(\bar{\phi}) &= \frac{J_1 - J_2}{J_1 + J_2} \cot(\delta\phi/2). \end{aligned} \quad (8)$$

The value of the potential at these minima is

$$V_{\min} = J_3 \frac{J_1^2 + J_2^2}{2J_1J_2} - \frac{J_1J_2}{2J_3}. \quad (9)$$

The classical equations of motion for the above Lagrangian (with $\Phi = \pi$) may be easily derived and rewritten as

$$\begin{aligned} \frac{\Phi_0^2}{8\pi^2 J} \hat{C} \begin{pmatrix} \ddot{\vec{\phi}} \\ \delta\dot{\vec{\phi}} \end{pmatrix} &= \begin{pmatrix} 1 & \epsilon \\ \epsilon & 1 \end{pmatrix} \begin{pmatrix} -\sin \bar{\phi} \sin \frac{\delta\phi}{2} \\ \cos \bar{\phi} \cos \frac{\delta\phi}{2} \end{pmatrix} \\ &\quad - \begin{pmatrix} 0 \\ \lambda \sin(\delta\phi) \end{pmatrix}, \end{aligned} \quad (10)$$

where we have defined $J_1 = (1 + \epsilon)J$, $J_2 = (1 - \epsilon)J$, $J_3 = \lambda J$,

$$\hat{C} = \begin{pmatrix} \tilde{C} & \tilde{C} \\ \tilde{C} & C_\delta \end{pmatrix}, \quad (11)$$

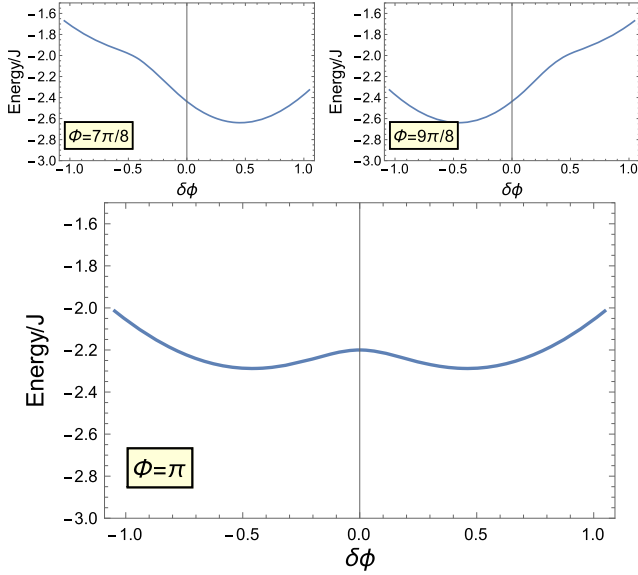


FIG. 5. Potential energy vs the superconducting phase difference $\delta\phi$ (minimized over the average superconducting phase $\bar{\phi}$) near the degeneracy point, plotted for a strong junction twice as strong as the average of the other two ($\lambda = 2$) and a Josephson asymmetry $\epsilon = 0.1$. Note that two inequivalent minima develop when the flux from the external field $\Phi = \pi$, and an instanton event is required for the system to remain in the absolute minimum of energy as Φ is tuned past this point. This instanton may occur either with a forward or a backward jump in $\bar{\phi}$, and there is interference between the two paths.

and

$$\bar{C} = C_1 + C_2 - 2C_3,$$

$$\tilde{C} = C_1 - C_2,$$

$$C_\delta = C_1 + C_2 + 2C_3.$$

We analyze these equations using an instanton approximation in the limit $\eta = [(1 - \epsilon^2)/(2\lambda)] \ll 1$. Note that the condition (7) additionally requires that $\epsilon < \eta$.

In this case, we can vastly simplify the equations of motion by expanding in orders of η :

$$\delta\phi = 2\eta \cos \bar{\phi} - \frac{\Phi_0^2 \tilde{C}}{4\pi^2 J} \ddot{\bar{\phi}} + \mathcal{O}(\eta^3). \quad (12)$$

To bound the order of the corrections, we have used the fact that the first equation of motion implies that time derivatives scale as $\sqrt{\eta}$ because the $\bar{\phi}$ excursion for the instanton is not small. Next, we make use of energy conservation to gain the first integral of motion:

$$H = 0 = \frac{\Phi_0^2}{8\pi^2 \bar{C}} (\bar{C} - \eta \tilde{C} \sin \bar{\phi})^2 \dot{\bar{\phi}}^2 + J\eta \left(\sin \bar{\phi} - \frac{\epsilon}{\eta} \right)^2 + \mathcal{O}(\eta^3). \quad (13)$$

Note that for this equation to have a nontrivial solution for real ϕ_i , we must propagate the system in imaginary time (hence the instanton solution). The total instanton action is therefore

$$S = \int_{-i\infty}^{i\infty} dt \sqrt{\frac{\Phi_0^2 J \eta}{2\pi^2 \bar{C}}} i(\bar{C} - \eta \tilde{C} \sin \bar{\phi}) \left(\sin \bar{\phi} - \frac{\epsilon}{\eta} \right) + \frac{\Phi_0}{2\pi} (Q_1 + Q_2 + eq) \dot{\bar{\phi}} + \frac{\Phi_0}{4\pi} (Q_1 - Q_2 + eq) \delta\dot{\bar{\phi}} + \mathcal{O}(\eta^3). \quad (14)$$

The last term provides a constant phase shift that is exactly canceled by the adiabatic phase coming from the change of the potential minimum for $\delta\phi$ as Φ is cycled from 0 to 2π (unlike $\bar{\phi}$, $\delta\phi$ returns to zero after a full cycle). Likewise, we may ignore terms that are independent of the direction that $\bar{\phi}$ travels. In fact, we are only interested in the difference between the action of the paths with positive and negative $\bar{\phi}$. The effective phase gate after adiabatic evolution of Φ is given by

$$U(q) = \exp(i \text{Arg}(1 + e^{i(S_+(q) - S_-(q))})), \quad (15)$$

where q is the qubit state and we can now calculate

$$S_+ - S_- = -i\Phi_0 \sqrt{\frac{J\eta}{2\bar{C}}} \left(2\bar{C} \frac{\epsilon}{\eta} + \eta \tilde{C} \right) + \mathcal{O}(\eta^{5/2}) + \Phi_0(Q_1 + Q_2) + \pi q. \quad (16)$$

Note that the phase gate given by Eq. (15) is gauge dependent. We have chosen the gauge in which tunneling a Josephson vortex through J_1 gives a π phase difference between the two states of the qubit, while tunneling a vortex through J_2 does not measure the qubit charge. In order to get a gauge-invariant quantity, we can reverse our procedure to release the vortex from the superconducting loop by ramping down the magnetic field, this time with J_2 tuned to 0 so that the vortex has a guaranteed exit path. We do not comment further on this second step of the procedure and simply make the preceding (equivalent) gauge choice in what follows.

The difference in instanton actions for the two entry paths takes the form $i(S_+ - S_-) = i\pi q + i\chi - d$, where χ and d are real numbers with $\chi = \Phi_0(Q_1 + Q_2)$ and $d \approx \Phi_0 \sqrt{[(J\eta)/(2\bar{C})]} [(2\bar{C}(\epsilon/\eta) + \eta \tilde{C})]$. In these terms, the phase accumulated between the two qubit states is given by

$$2\theta = \arg[\sinh(d) + i \sin(\chi)]. \quad (17)$$

The $\pi/8$ phase gate appropriate to magic-state distillation [23], or for maximizing the violation of the CHSH

inequality [see Eqs. (2) and (3)], may be attained by choosing, e.g., $\chi = \pi/2$, $d = \text{asinh}(1)$.

One possible source of error is an induced splitting between the qubit states due to different rates of tunneling for the two qubit states near the instanton point $\Phi = \pi$, leading to a dynamic phase error in the qubit. Near the instanton point, the wave function is in a superposition between the left and right minima, and the energy of the lower state depends on the probability of the instanton event occurring. If this probability is different for different qubit states, the qubit will split. The probability of the instanton event occurring for each state is proportional to

$$P(q) \propto |1 + e^{i(S_+(q) - S_-(q))}| = |1 + (-1)^q e^{-d + i\chi}|. \quad (18)$$

This splitting puts a lower bound on how fast the phase gate should be performed, so as to minimize the accumulation of phase error. Note that if $\chi = \pi/2$, there is no splitting, as the probabilities are equal for the two qubit states. [This is also the condition that maximizes the controlled phase given by Eq. (17)]. We expect the dynamic phase error to be minimized under this condition, an expectation that is (approximately) borne out by our numerical calculation.

In the next section, we present the results of a numerical calculation that supports the analytical instanton analysis of this section.

IV. NUMERICAL SIMULATION

In order to go beyond the instanton approximation detailed in the previous section, we performed numerical simulations of the Schrodinger equation associated with the Lagrangian (5). The corresponding Hamiltonian for the system can be written as

$$H(\Phi) = E_C \sum_{j=1,2} \left(n_j - \frac{Q_j}{2e} \right)^2 - J_1 \cos(\phi_1) - J_2 \cos(\phi_2 + \Phi) - J_3 \cos(\phi_1 - \phi_2), \quad (19)$$

where E_C is the charging energy of each island (here, we assume $C_1 = C_2 = 2e^2/E_C$, $C_3 = 0$ for simplicity) and $n_j = -i\partial_{\phi_j}$ is the charge operator on each superconducting island. The Josephson energy part of the Hamiltonian, which is proportional to $J_{1,2,3}$, is identical to the potential used in the Lagrangian in Eq. (6) up to a gauge transformation. For the numerical calculation, it is convenient to choose a gauge where the Hamiltonian is manifestly 2π periodic. Technically, there are three different such gauges where the flux enters across each of the junctions. As mentioned at the end of the last section, invariance with respect to the different gauge choices is guaranteed only when the Hamiltonian traces a closed loop where the flux Φ vanishes at the beginning and the end of the loop.

In order to perform the simulation of the phase gate process, we divide the process of changing the flux Φ through the loop from 0 to 2π into a series of small time

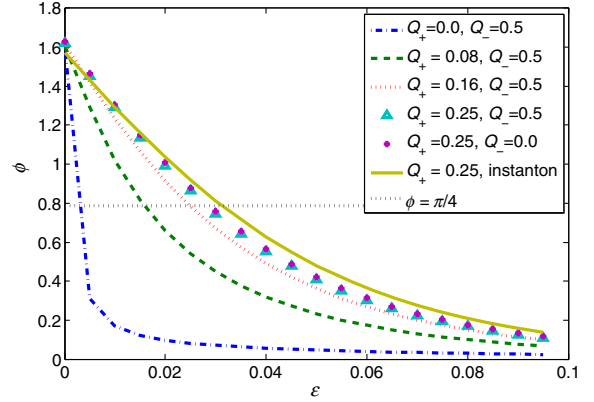


FIG. 6. The relative phase acquired between states of the qubit after the phase gate is enacted, here plotted as a function of the Josephson junction asymmetry ϵ for a strong junction that is twice as strong as the weak junctions ($\lambda = 2$). The charging energy E_C has been chosen to be 0.4 relative to the scale of the Josephson energy $(J_1 + J_2)/2$. The sum and difference of the gate charges [$Q_+ = (Q_1 + Q_2)$ and $Q_- = Q_1 - Q_2$] are expressed in units of the Cooper pair charge $2e$. Note that a relatively small junction asymmetry of $\epsilon \leq 0.1$ can tune the gate through a large range of phases.

steps. At each step, we numerically solve the Schrodinger equation $H(\Phi)|\psi(\Phi)\rangle = E(\Phi)|\psi(\Phi)\rangle$ by expanding the wave function in the eigenbasis $|n_1, n_2\rangle$ of the charge operators. The charging energy is diagonal in this basis, and the Josephson energy terms are represented in terms of “hopping” terms such as $|n_1, n_2\rangle\langle n_1 + 1, n_2|$, etc. Choosing a large enough cutoff ($n_j \in [-15, 15]$ turns out to be sufficient for our parameters), we can diagonalize the Hamiltonian matrix in the charge basis to obtain the ground-state wave function. Since the Hamiltonian is 2π periodic in the flux, the Berry phase can be computed from the expression

$$e^{i\theta_{\text{Berry}}} \approx \prod_{n=1}^N \left\langle \psi \left(\frac{2\pi n}{N} \right) \middle| \psi \left(\frac{2\pi(n+1)}{N} \right) \right\rangle, \quad (20)$$

where N is the number of steps into which we discretize the flux. Note that if we choose N to be too small, the magnitude of the right-hand side will be significantly less than unity, while as $N \rightarrow \infty$, the above approximation becomes exact [61]. The magnitude of the overlap at each step is thus an important diagnostic of the algorithm and should be near unity, serving as an important check on the accuracy of our simulation.

Figure 6 shows the relative phase between the two qubit states acquired through the adiabatic evolution. Note that the “magic” phase $\pi/4$ [23] can be attained either by adjusting the gate voltages to change Q_i or by adjusting the imbalance ϵ in the Josephson couplings. We can compare these results to the prediction of the instanton approximation using our calculated $d \approx 4\pi \sqrt{\{(\lambda J)/[E_C(1 - \epsilon^2)]\}}\epsilon$.

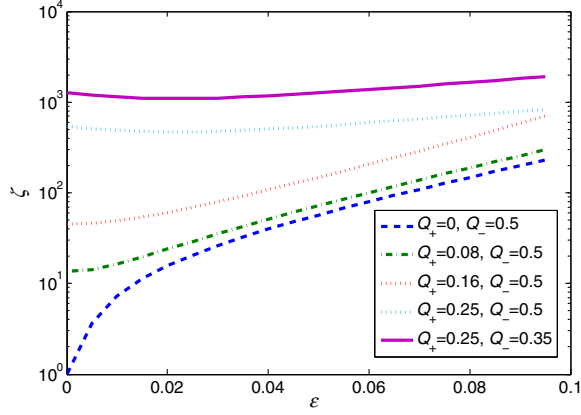


FIG. 7. The dynamical range of the phase gate as a function of the Josephson asymmetry ϵ for a set of gate charge values $Q_+ = (Q_1 + Q_2)$ and $Q_- = Q_1 - Q_2$ (expressed in units of $2e$). The best dynamic range is found for $Q_1 + Q_2 = 1/4$, corresponding to a phase of $\chi = \pi/2$ in Eq. (18). Here, the dynamic phase error and the minimal gap differ by 3 orders of magnitude, allowing the gate to function for a significant range of ramping times.

The qubit state q is encoded in the Hamiltonian through a shift of the gate charge $Q_1 \rightarrow Q_1 + q$. The qubit phase generated from the phase gate is found by calculating the difference of Berry phases $\theta_{\text{Berry}}(q=1) - \theta_{\text{Berry}}(q=0)$ acquired as the flux Φ is changed by 2π . To maintain adiabaticity, the flux must be swept at a rate that is small compared to the first excitation gap E_{gap} above the ground state $|\psi(\Phi)\rangle$ of the Hamiltonian in Eq. (19). Such a slow sweep rate leads to a dynamical contribution to the qubit phase that is given by

$$\theta_{\text{dyn}} = \int d\Phi \frac{E(\Phi, q=1) - E(\Phi, q=0)}{\dot{\Phi}}. \quad (21)$$

To keep this error small, the sweep rate $\dot{\Phi}$ must be kept larger than the energy difference, i.e., $|E(\Phi, q=1) - E(\Phi, q=0)| \ll \dot{\Phi}$. At the same time, adiabaticity requires $\dot{\Phi} \ll E_{\text{gap}}$. Thus, the dynamical range (i.e., the range of sweep rates) over which this gate can operate, is proportional to

$$\zeta = \frac{E_{\text{gap}}}{|E(\Phi, q=1) - E(\Phi, q=0)|}. \quad (22)$$

The inverse of the dynamical range ζ^{-1} also quantifies the contribution of the dynamical phase to the systematic error in the gate.

While at the lowest-order instanton approximation, the energy $E(\Phi, q)$ is independent of q , as seen from the numerical results in Fig. 7, higher-order instanton corrections lead to energy splittings that are a finite fraction $\zeta^{-1} > 0$ of the gap. This is apparent from Fig. 7 since in the ideal case ζ would be infinite. However, it is also clear that the leading-order contribution to ζ can be minimized by

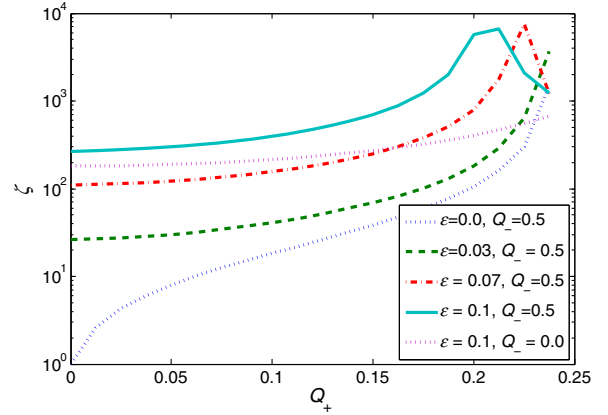


FIG. 8. The dynamical range of the phase gate as a function of the total gate charge $Q_+ = (Q_1 + Q_2)$ (units of $2e$) for a set of values of the Josephson asymmetry ϵ and $Q_- = Q_1 - Q_2$ (expressed in units of $2e$). Note the resonances in the dynamic range as the qubit states are tuned to degeneracy.

choosing the total gate charge near $Q_1 + Q_2 = 0.25$. This is expected if the major contribution to the qubit splitting comes from the instanton contribution described in Sec. III. Here, $Q_1 + Q_2 = 0.25$ corresponds to $\chi = \pi/2$ in Eq. (18). Figure 8 shows that the resonance in the dynamic range (corresponding to the degeneracy point for the qubit states) does not always occur exactly at $Q_1 + Q_2 = 0.25$. Higher-order corrections to the instanton calculation will detect the asymmetry in the system, leading to dependence of the resonance on $Q_1 - Q_2$ and ϵ . Nevertheless, it is evident that a dynamic range of 2–3 orders of magnitude is achievable over a broad range of parameter space, enabling a rather unconstrained experimental implementation of the phase gate without undue fine-tuning. Based on these results, in the next section we suggest a precise experimental scheme to implement our proposed phase gate as well as to verify the CHSH-Bell inequality mentioned in the title of our paper.

V. EXPERIMENTAL PROPOSAL

In order to implement and test this phase gate within a physical system, we turn to the measurement scheme proposed by Hassler *et al.* [32] (and used extensively by Hyart *et al.* [33]) in which the parity of a pair of Majorana fermions is read out through a superconducting charge qubit in a transmission line resonator (a “transmon” [62]). Using the arrangement shown in Fig. 9, we can implement all of the steps of the CHSH-Bell test without ever needing to physically braid any of the Majoranas. This is in line with the so-called “measurement-only” schemes for topological quantum computation [26,27]. In our proposed experiment, each of the islands containing Majorana wires is attached through a series of adjustable Josephson junctions to the larger superconducting region on either the top (bus) or bottom (phase ground). We assume that the coupling

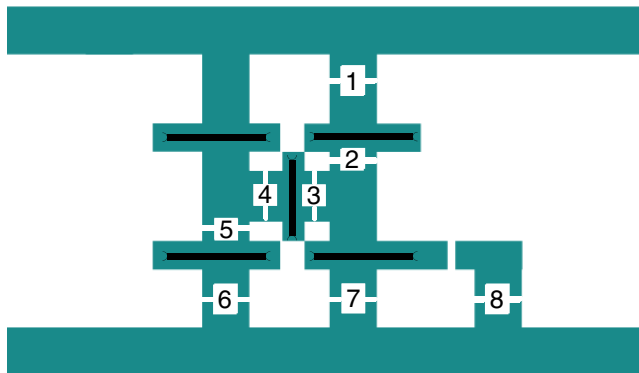


FIG. 9. Experimental design for CHSH measurement. The system consists of several superconducting islands placed within a microwave resonator. Five Majorana nanowires are placed among the islands in such a way as to produce six Majorana zero modes, one at each endpoint along the outer edge, and one at each intersection where three wires meet [33]. The top three Majoranas form one qubit, and the bottom three another. Eight adjustable Josephson junctions (and one strong fixed junction) couple the islands to each other and to the bus (top) and phase ground (bottom) of the microwave resonator. Of these junctions, those labeled 1–6 need only have “on” (strongly coupled) and “off” (very weakly coupled) settings. Junctions 7 and 8 are used to implement the phase gate as described in the main text.

between the three Majoranas at each of the trijunctions is strong compared with the charging energy of the islands and is comparable to the Josephson energy at junction J_8 during the performance of the phase gate. Because of this large coupling, the Majorana at the left end of the wire in Fig. 3 is effectively replaced by the zero mode of the trijunction.

Measurement of the resonance frequency of this system when placed within a microwave resonator can resolve whether the total parity of islands connected to the bus is even or odd [31,33,62]. Again, the trijunction coupling is assumed to be large compared with the measurement scale so that the trijunctions are treated as effectively single MZMs. The X and Z components of the upper qubit may be measured by connecting the islands containing the corresponding MZMs strongly to the bus (while connecting all other islands to the phase ground; see Fig. 11). Similarly, measurements of the lower qubit may be made by strongly connecting the corresponding islands to the phase ground (Fig. 12). Because the resonator measurement determines the total parity connected to the bus, the parity of the islands connected to the phase ground may be inferred once the overall parity of the Majorana system is measured. We label this a “tare” measurement (see Fig. 10).

Together, Figs. 10–12 show the sets of islands coupled to the bus and phase ground corresponding to each of the measurements necessary for a test of the CHSH inequality. In most cases, we need only two settings for our Josephson junctions, a strong connection $E_J \gg E_C$ (on) and a very

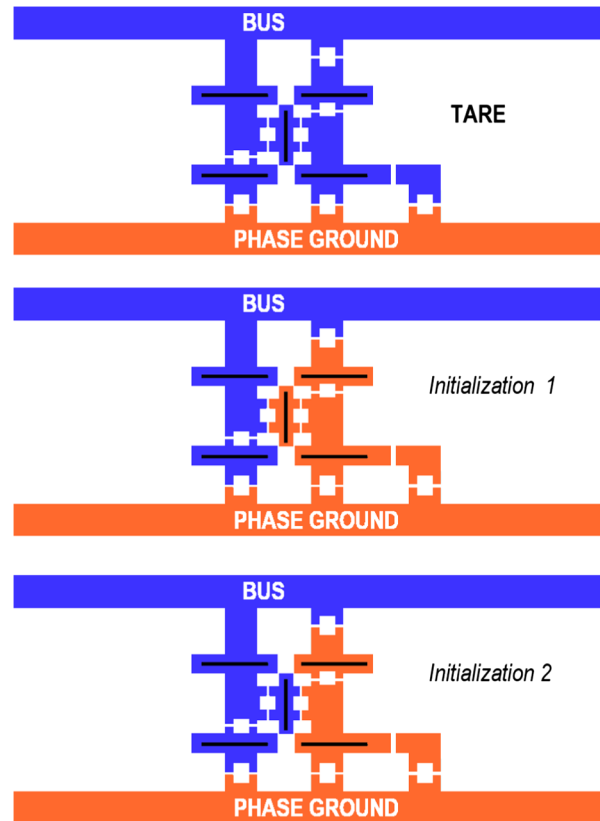


FIG. 10. Initialization process. The blue (dark gray) and orange (light gray) superconducting islands are strongly Josephson coupled to the bus and phase ground, respectively. (Top) Coupling all islands to the bus gives a measurement of the overall fermion parity of the system. This allows one to equivalently measure the parity of a qubit by coupling the constituent Majorana modes to the bus or the phase ground. (Middle and bottom) The two qubits in this device may be put into the superposition $(1/\sqrt{2})(|00\rangle + |11\rangle)$ by making two measurements; each measurement includes one MZM from each qubit. (Along with the tare measurement, this will also effectively measure the parity of the central island.)

weak connection $E_J \ll E_C$ (off). This switching can be controlled, e.g., by threading half a flux between two strong Josephson junctions [33]. The two Josephson junctions in the lower right of Fig. 9, labeled 7 and 8, adjust the phase gate in the manner described above, acting as control parameters for J_1 and J_2 . A strong Josephson coupling J_3 is assumed between the two islands in the lower right. While the phase gate is being implemented, junctions 2 and 3 should be off, allowing flux to pass freely between the island containing the lower right Majorana wire (“ y ”) and the remaining wires. The loop in the lower right now acts as the superconducting loop of Fig. 3 for implementing the phase gate around the y axis. The remaining Josephson junctions should be on so that no measurement path is open in the resonator system and all other islands have the superconducting phase inherited from the phase ground. In this case, the Josephson energy of the lower trijunction acts

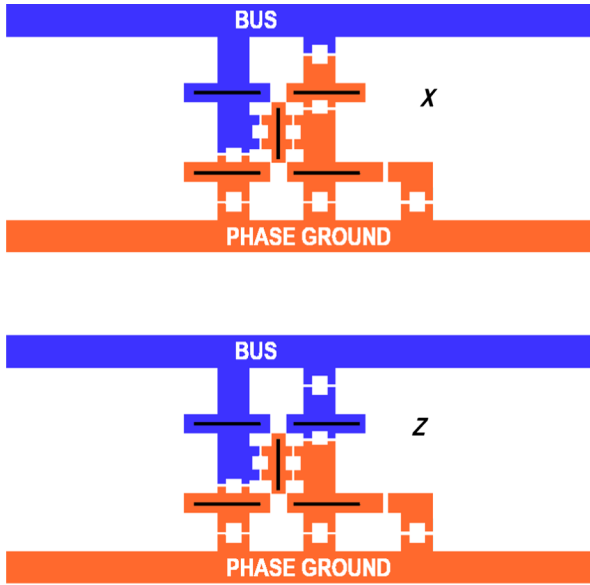


FIG. 11. Measurement of the X and Z projections of the upper qubit. The parity of a set of MZMs is measured by Josephson coupling the corresponding superconducting islands strongly to the bus while coupling the remaining islands to the phase ground.

to renormalize the coupling J_1 in the phase gate design of Fig. 3.

Figures 9–12 provide the schematic and the protocol for the experimental platform as well as the necessary measurements for the phase gate and CHSH violation being introduced in this work. They also provide all the tools necessary to conduct an independent test of the fidelity of

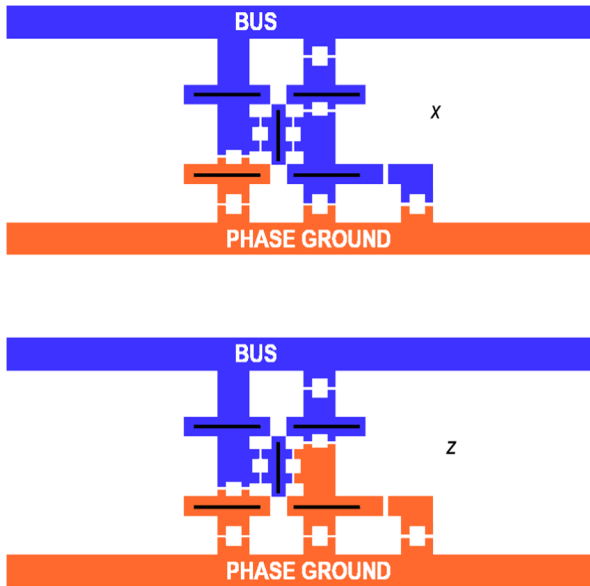


FIG. 12. Measurement of the x and z projections of the lower qubit. The tare measurement (see Fig. 10) allows one to relate the parity of the section coupled to the phase ground to the parity of the section coupled to the bus.

the phase gate without any alteration of the device, e.g., by measuring x before and after a phase rotation around y .

VI. QUBIT DESIGN FOR UNIVERSAL QUANTUM COMPUTATION

Once Bell violations have been demonstrated, the next step toward universal quantum computation is a scalable qubit register in which all necessary gate operations (e.g., Clifford gates and the $\pi/8$ phase gate) could be performed. Our phase gate may be easily worked into such a design, as we demonstrate here in a simplification of the random access Majorana memory (RAMM) introduced in Ref. [33].

As shown in Fig. 13, we can construct a set of islands within the resonator system to function as a single qubit, with measurement settings available to measure any Pauli operator $\{I, X, Y, Z\}$, along with a phase gate that operates around the Y axis. Furthermore, by coupling several qubits to the same register, we may perform *any* Pauli measurement on the qubits. As described in Refs. [26,27], the set of Clifford gates may be efficiently constructed using Pauli measurements. Combined with the phase gates available on each qubit and the distillation of magic states [23] using these phase gates, this design provides the necessary components for universal quantum computation. One important feature of this new design is the elimination of a need for nanowire “networks.” Only a single (and separated) crossing of Majorana wires is needed for each qubit, significantly simplifying the fabrication of the Majorana register. We believe that the method outlined in our Fig. 13, which combines magic-state distillation and measurement-only ideas in the context of our proposed phase gate, may very well be the most practical experimental way yet proposed for carrying out universal quantum computation using nanowire MZMs.

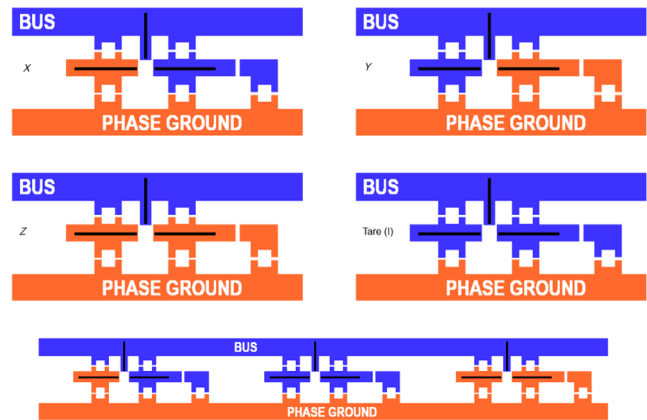


FIG. 13. Top four panels: Qubit design showing measurement configurations for X , Y , Z , and Tare (I) measurements of a qubit. Bottom panel: Portion of a RAMM in a configuration measuring $X \otimes I \otimes Z$.

VII. OUTLOOK

The novel phase gate described in this paper should more than meet the threshold for error correction in carrying out universal fault-tolerant quantum computation using MZMs [23]. The real-world function of the phase gate, as well as its quantum entanglement properties (beyond the Gottesmann-Knill constraint of pure Clifford operations), can be diagnosed through Bell measurements. These tests of the CHSH inequality are no more daunting than tests of braiding, yet are better targeted toward the eventual implementation of quantum information processing in Majorana-based platforms. In fact, it has been shown that any operation capable of producing a violation of the CHSH inequality, when combined with Clifford operations, is sufficient for universal quantum computation [28]. By contrast, we do not envision our proposed experiments as tests of quantum nonlocality itself, as it is unlikely that the qubits in our proposal will be spacelike separated. In any case, it is clear that nonlocality is not sufficient for universal quantum computation, as it may be achieved in Ising anyons through braiding alone [63] (a system that does not even suffice for universal classical computation). The role of the CHSH inequalities as a benchmark in Ising or Majorana systems has been explored before [28,64–66]. Here, we propose to use this benchmark to experimentally characterize the new phase gate realization we have put forth, a realization that benefits from a relative immunity to timing errors and that can be combined with measurement operations in a unified architecture.

We believe that our proposal is simple enough, and the consequences of an experimental implementation important enough, that serious consideration should be given by experimentalists toward trying this Bell violation experiment as the very first quantum entanglement experiment in the semiconductor Majorana wire system, even before garden-variety braiding experiments are performed. We note here with considerable relief that our phase-gate idea leads to a precise test for Bell violation as well as a well-defined platform for universal fault-tolerant quantum computation on more or less the same footing, using platforms very similar to those currently being constructed in laboratories for nanowire MZM braiding experiments.

ACKNOWLEDGMENTS

We are grateful to Kirill Shtengel for suggesting Bell violations as a diagnostic tool. This work is supported by Microsoft Station Q and LPS-CMTC.

[1] D. Gottesman, in *Proceedings of the XXII International Colloquium on Group Theoretical Methods in Physics*, edited by S.P. Corney, R. Delbourgo, and P.D. Jarvis (International Press, Cambridge, 1999), pp. 32–43.

- [2] M. E. Cuffaro, *On the Significance of the Gottesman-Knill Theorem*, [arXiv:1310.0938](https://arxiv.org/abs/1310.0938).
- [3] M. Freedman, A. Kitaev, M. Larsen, and Z. Wang, *Topological Quantum Computation*, *Bull. Am. Math. Soc.* **40**, 31 (2003).
- [4] C. Nayak, S. H. Simon, A. Stern, M. Freedman, and S. Das Sarma, *Non-Abelian Anyons and Topological Quantum Computation*, *Rev. Mod. Phys.* **80**, 1083 (2008).
- [5] J. S. Bell, *On the Einstein Poldolsky Rosen Paradox*, *Physics* **3**, 195 (1964).
- [6] J. F. Clauser, M. A. Horne, A. Shimony, and R. A. Holt, *Proposed Experiment to Test Local Hidden-Variable Theories*, *Phys. Rev. Lett.* **23**, 880 (1969).
- [7] J. Alicea, *New Directions in the Pursuit of Majorana Fermions in Solid State Systems*, *Rep. Prog. Phys.* **75**, 076501 (2012).
- [8] M. Leijnse and K. Flensberg, *Introduction to Topological Superconductivity and Majorana Fermions*, *Semicond. Sci. Technol.* **27**, 124003 (2012).
- [9] C. W. J. Beenakker, *Search for Majorana Fermions in Superconductors*, *Annu. Rev. Condens. Matter Phys.* **4**, 113 (2013).
- [10] T. D. Stanescu and S. Tewari, *Majorana Fermions in Semiconductor Nanowires: Fundamentals, Modeling, and Experiment*, *J. Phys. Condens. Matter* **25**, 233201 (2013).
- [11] S. Das Sarma, M. Freedman, and C. Nayak, *Majorana Zero Modes and Topological Quantum Computation*, *Quantum Information* **1**, 15001 (2015).
- [12] S. R. Elliott and M. Franz, *Colloquium: Majorana Fermions in Nuclear, Particle, and Solid-State Physics*, *Rev. Mod. Phys.* **87**, 137 (2015).
- [13] A. G. Fowler, M. Mariantoni, J. M. Martinis, and A. N. Cleland, *Surface Codes: Towards Practical Large-Scale Quantum Computation*, *Phys. Rev. A* **86**, 032324 (2012).
- [14] R. Barends, J. Kelly, A. Megrant, A. Veitia, D. Sank, E. Jeffrey, T. C. White, J. Mutus, A. G. Fowler, B. Campbell *et al.*, *Superconducting Quantum Circuits at the Surface Code Threshold for Fault Tolerance*, *Nature (London)* **508**, 500 (2014).
- [15] P. Bonderson, S. Das Sarma, M. Freedman, and C. Nayak, *A Blueprint for a Topologically Fault-Tolerant Quantum Computer*, [arXiv:1003.2856](https://arxiv.org/abs/1003.2856).
- [16] R. S. K. Mong, D. J. Clarke, J. Alicea, N. H. Lindner, P. Fendley, C. Nayak, Y. Oreg, A. Stern, E. Berg, K. Shtengel, and M. P. A. Fisher, *Universal Topological Quantum Computation from a Superconductor-Abelian Quantum Hall Heterostructure*, *Phys. Rev. X* **4**, 011036 (2014).
- [17] E. M. Stoudenmire, D. J. Clarke, R. S. K. Mong, and J. Alicea, *Assembling Fibonacci Anyons from a Z_3 Parafermion Lattice Model*, *Phys. Rev. B* **91**, 235112 (2015).
- [18] M. Barkeshli, C.-M. Jian, and X.-L. Qi, *Twist Defects and Projective Non-Abelian Braiding Statistics*, *Phys. Rev. B* **87**, 045130 (2013).
- [19] M. Barkeshli, P. Bonderson, M. Cheng, and Z. Wang, *Symmetry, Defects, and Gauging of Topological Phases*, [arXiv:1410.4540](https://arxiv.org/abs/1410.4540).
- [20] V. Kliuchnikov, A. Bocharov, and K. M. Svore, *Asymptotically Optimal Topological Quantum Compiling*, *Phys. Rev. Lett.* **112**, 140504 (2014).

- [21] B. M. Terhal, *Quantum Error Correction for Quantum Memories*, *Rev. Mod. Phys.* **87**, 307 (2015).
- [22] M. Freedman, C. Nayak, and K. Walker, *Towards Universal Topological Quantum Computation in the $\nu = 5/2$ Fractional Quantum Hall State*, *Phys. Rev. B* **73**, 245307 (2006).
- [23] S. Bravyi and A. Kitaev, *Universal Quantum Computation with Ideal Clifford Gates and Noisy Ancillas*, *Phys. Rev. A* **71**, 022316 (2005).
- [24] G. Duclos-Cianci and D. Poulin, *Reducing the Quantum-Computing Overhead with Complex Gate Distillation*, *Phys. Rev. A* **91**, 042315 (2015).
- [25] C. Knapp, M. Zaletel, D. E. Liu, M. Cheng, P. Bonderson, and C. Nayak, *How Quickly Can Anyons Be Braided? Or: How I Learned to Stop Worrying About Adiabatic Errors and Love the Anyon*, arXiv:1601.05790.
- [26] P. Bonderson, M. Freedman, and C. Nayak, *Measurement-Only Topological Quantum Computation*, *Phys. Rev. Lett.* **101**, 010501 (2008).
- [27] P. Bonderson, M. Freedman, and C. Nayak, *Measurement-Only Topological Quantum Computation via Anyonic Interferometry*, *Ann. Phys. (Amsterdam)* **324**, 787 (2009).
- [28] M. Howard and J. Vala, *Nonlocality as a Benchmark for Universal Quantum Computation in Ising Anyon Topological Quantum Computers*, *Phys. Rev. A* **85**, 022304 (2012).
- [29] P. Bonderson, D. J. Clarke, C. Nayak, and K. Shtengel, *Implementing Arbitrary Phase Gates with Ising Anyons*, *Phys. Rev. Lett.* **104**, 180505 (2010).
- [30] D. J. Clarke and K. Shtengel, *Improved Phase-Gate Reliability in Systems with Neutral Ising Anyons*, *Phys. Rev. B* **82**, 180519 (2010).
- [31] F. Hassler, A. R. Akhmerov, C.-Y. Hou, and C. W. J. Beenakker, *Anyonic Interferometry without Anyons: How a Flux Qubit Can Read out a Topological Qubit*, *New J. Phys.* **12**, 125002 (2010).
- [32] F. Hassler, A. R. Akhmerov, and C. W. J. Beenakker, *The Top-Transmon: A Hybrid Superconducting Qubit for Parity-Protected Quantum Computation*, *New J. Phys.* **13**, 095004 (2011).
- [33] T. Hyart, B. van Heck, I. C. Fulga, M. Burrello, A. R. Akhmerov, and C. W. J. Beenakker, *Flux-Controlled Quantum Computation with Majorana Fermions*, *Phys. Rev. B* **88**, 035121 (2013).
- [34] J. D. Sau, S. Tewari, and S. Das Sarma, *Universal Quantum Computation in a Semiconductor Quantum Wire Network*, *Phys. Rev. A* **82**, 052322 (2010).
- [35] J. D. Sau, D. J. Clarke, and S. Tewari, *Controlling Non-Abelian Statistics of Majorana Fermions in Semiconductor Nanowires*, *Phys. Rev. B* **84**, 094505 (2011).
- [36] J. Alicea, Y. Oreg, G. Refael, F. von Oppen, and M. P. A. Fisher, *Non-Abelian Statistics and Topological Quantum Information Processing in 1D Wire Networks*, *Nat. Phys.* **7**, 412 (2011).
- [37] B. van Heck, A. R. Akhmerov, F. Hassler, M. Burrello, and C. W. J. Beenakker, *Coulomb-Assisted Braiding of Majorana Fermions in a Josephson Junction Array*, *New J. Phys.* **14**, 035019 (2012).
- [38] L. P. Kouwenhoven (private communication).
- [39] C. M. Marcus (private communication).
- [40] D. J. Clarke, J. Alicea, and K. Shtengel, *Exotic Non-Abelian Anyons from Conventional Fractional Quantum Hall States*, *Nat. Commun.* **4**, 1348 (2013).
- [41] N. H. Lindner, E. Berg, G. Refael, and A. Stern, *Fractionalizing Majorana Fermions: Non-Abelian Statistics on the Edges of Abelian Quantum Hall States*, *Phys. Rev. X* **2**, 041002 (2012).
- [42] M. Cheng, *Superconducting Proximity Effect on the Edge of Fractional Topological Insulators*, *Phys. Rev. B* **86**, 195126 (2012).
- [43] If the “wrong” state is obtained, it may be corrected by measuring one MZM from the pair with one outside and then repeated until success is achieved [26].
- [44] P. Bonderson and R. M. Lutchyn, *Topological Quantum Buses: Coherent Quantum Information Transfer between Topological and Conventional Qubits*, *Phys. Rev. Lett.* **106**, 130505 (2011).
- [45] P. Bonderson, L. Fidkowski, M. Freedman, and K. Walker, *Twisted Interferometry*, arXiv:1306.2379.
- [46] In many ways, what we describe is a practical implementation of the fine-tuned interferometry described in Ref. [45].
- [47] V. Mourik, K. Zuo, S. M. Frolov, S. R. Plissard, E. P. A. M. Bakkers, and L. P. Kouwenhoven, *Signatures of Majorana Fermions in Hybrid Superconductor-Semiconductor Nanowire Devices*, *Science* **336**, 1003 (2012).
- [48] A. Das, Y. Ronen, Y. Most, Y. Oreg, M. Heiblum, and H. Shtrikman, *Zero-Bias Peaks and Splitting in an Al-InAs Nanowire Topological Superconductor as a Signature of Majorana Fermions*, *Nat. Phys.* **8**, 887 (2012).
- [49] M. T. Deng, C. L. Yu, G. Y. Huang, M. Larsson, P. Caroff, and H. Q. Xu, *Anomalous Zero-Bias Conductance Peak in a Nb-InSb Nanowire-Nb Hybrid Device*, *Nano Lett.* **12**, 6414 (2012).
- [50] L. P. Rokhinson, X. Liu, and J. K. Furdyna, *The Fractional a.c. Josephson Effect in a Semiconductor-Superconductor Nanowire as a Signature of Majorana Particles*, *Nat. Phys.* **8**, 795 (2012).
- [51] A. D. K. Finck, D. J. Van Harlingen, P. K. Mohseni, K. Jung, and X. Li, *Anomalous Modulation of a Zero-Bias Peak in a Hybrid Nanowire-Superconductor Device*, *Phys. Rev. Lett.* **110**, 126406 (2013).
- [52] H. O. H. Churchill, V. Fatemi, K. Grove-Rasmussen, M. T. Deng, P. Caroff, H. Q. Xu, and C. M. Marcus, *Superconductor-Nanowire Devices from Tunneling to the Multichannel Regime: Zero-Bias Oscillations and Magnetocconductance Crossover*, *Phys. Rev. B* **87**, 241401 (2013).
- [53] W. Chang, S. M. Albrecht, T. S. Jespersen, F. Kuemmeth, P. Krogstrup, J. Nygård, and C. M. Marcus, *Hard Gap in Epitaxial Superconductor-Semiconductor Nanowires*, *Nat. Nanotechnol.* **10**, 232 (2015).
- [54] R. M. Lutchyn, J. D. Sau, and S. Das Sarma, *Majorana Fermions and a Topological Phase Transition in Semiconductor-Superconductor Heterostructures*, *Phys. Rev. Lett.* **105**, 077001 (2010).
- [55] Y. Oreg, G. Refael, and F. von Oppen, *Helical Liquids and Majorana Bound States in Quantum Wires*, *Phys. Rev. Lett.* **105**, 177002 (2010).
- [56] J. D. Sau, S. Tewari, R. M. Lutchyn, T. D. Stanescu, and S. Das Sarma, *Non-Abelian Quantum Order in Spin-Orbit-Coupled Semiconductors: Search for Topological*

- Majorana Particles in Solid-State Systems*, *Phys. Rev. B* **82**, 214509 (2010).
- [57] Y. Aharonov and A. Casher, *Topological Quantum Effects for Neutral Particles*, *Phys. Rev. Lett.* **53**, 319 (1984).
- [58] W. J. Elion, J. J. Wachtters, L. L. Sohn, and J. E. Mooij, *Observation of the Aharonov-Casher Effect for Vortices in Josephson-Junction Arrays*, *Phys. Rev. Lett.* **71**, 2311 (1993).
- [59] M. König, A. Tschetschetkin, E. M. Hankiewicz, Jairo Sinova, V. Hock, V. Daumer, M. Schäfer, C. R. Becker, H. Buhmann, and L. W. Molenkamp, *Direct Observation of the Aharonov-Casher Phase*, *Phys. Rev. Lett.* **96**, 076804 (2006).
- [60] E. Grosfeld and A. Stern, *Observing Majorana Bound States of Josephson Vortices in Topological Superconductors*, *Proc. Natl. Acad. Sci. U.S.A.* **108**, 11810 (2011).
- [61] R. Resta, *Macroscopic Polarization in Crystalline Dielectrics: The Geometric Phase Approach*, *Rev. Mod. Phys.* **66**, 899 (1994).
- [62] J. Koch, T. M. Yu, J. Gambetta, A. A. Houck, D. I. Schuster, J. Majer, A. Blais, M. H. Devoret, S. M. Girvin, and R. J. Schoelkopf, *Charge-Insensitive Qubit Design Derived from the Cooper Pair Box*, *Phys. Rev. A* **76**, 042319 (2007).
- [63] E. T. Campbell, M. J. Hoban, and J. Eisert, *Majorana Fermions and Non-Locality*, *Quantum Inf. Comput.* **14**, 0981 (2014).
- [64] C. Zhang, S. Tewari, and S. Das Sarma, *Bell's Inequality and Universal Quantum Gates in a Cold-Atom Chiral Fermionic p -wave Superfluid*, *Phys. Rev. Lett.* **99**, 220502 (2007).
- [65] G. K. Brennen, S. Iblisdir, J. K. Pachos, and J. K. Slingerland, *Non-Locality of Non-Abelian Anyons*, *New J. Phys.* **11**, 103023 (2009).
- [66] D. E. Drummond, A. A. Kovalev, C.-Y. Hou, K. Shtengel, and L. P. Pryadko, *Demonstrating Entanglement by Testing Bell's Theorem in Majorana Wires*, *Phys. Rev. B* **90**, 115404 (2014).